

## Supplementary Information for

**HCC EV ECG Score: An Extracellular Vesicle-based Protein Assay for  
Detection of Early-Stage Hepatocellular Carcinoma**

Na Sun,<sup>1,2,†</sup> Ceng Zhang,<sup>1,3,†</sup> Yi-Te Lee,<sup>1,†</sup> Benjamin V. Tran,<sup>4</sup> Jing Wang,<sup>1</sup> Hyoyong Kim,<sup>1</sup> Junseok Lee,<sup>1</sup> Ryan Y. Zhang,<sup>1</sup> Jasmine J. Wang,<sup>1,5</sup> Junhui Hu,<sup>6</sup> Zhicheng Zhang,<sup>6</sup> Manaf S. Alsudaney,<sup>7</sup> Kuan-Chu Hou,<sup>1</sup> Hubert Tang,<sup>1</sup> Tiffany X. Zhang,<sup>1</sup> Icy Y. Liang,<sup>1</sup> Ziang Zhou,<sup>1</sup> Mengxiang Chen,<sup>1</sup> Angela Hsiao-Jiun Yeh,<sup>8</sup> Wenyuan Li,<sup>9</sup> Xianghong Jasmine Zhou,<sup>9</sup> Helena R. Chang,<sup>4</sup> Steven-Huy B. Han,<sup>8</sup> Saeed Sadeghi,<sup>8</sup> Richard S. Finn,<sup>8</sup> Sammy Saab,<sup>8</sup> Ronald W. Busuttil,<sup>4</sup> Mazen Nouredin,<sup>7,10</sup> Walid S. Ayoub,<sup>7,10</sup> Alexander Kuo,<sup>7,10</sup> Vinay Sundaram,<sup>7,10</sup> Buraq Al-Ghaieb,<sup>7,10</sup> Juvelyn Palomique,<sup>7</sup> Kambiz Kosari,<sup>7</sup> Irene K. Kim,<sup>7</sup> Tsuyoshi Todo,<sup>7</sup> Nicholas N. Nissen,<sup>7</sup> Maria Lauda Tomasi,<sup>10</sup> Sungyong You,<sup>11</sup> Edwin M. Posadas,<sup>5</sup> James X. Wu,<sup>4</sup> Madhuri Wadehra,<sup>9</sup> Myung-Shin Sim,<sup>12</sup> Yunfeng Li,<sup>9</sup> Hanlin L. Wang,<sup>9</sup> Samuel W. French,<sup>9</sup> Shelly C. Lu,<sup>10,13</sup> Lily Wu,<sup>6</sup> Renjun Pei,<sup>2\*</sup> Li Liang,<sup>14,15\*</sup> Ju Dong Yang,<sup>7,10,13\*</sup> Vatche G. Agopian,<sup>4,16\*</sup> Hsian-Rong Tseng<sup>1,16\*</sup> and Yazhen Zhu<sup>1,9,16\*</sup>

†These authors contributed equally to this work.

\*Corresponding authors

To whom correspondence should be addressed. e-mail: rjpei2011@sinano.ac.cn (R.P.); lli@smu.edu.cn (L.L.); JuDong.Yang@cshs.org (J.D.Y.); vagopian@mednet.ucla.edu (V.G.A.); hrtseng@mednet.ucla.edu (H.-R.T.); yazhenzhu@mednet.ucla.edu (Y.Z.).

**This PDF file includes:**

## **SUPPLEMENTARY METHODS**

### **SUPPLEMENTARY FIGURES**

- Fig. S1. Fabrication of Click Beads
- Fig. S2. Characterization of HCC cell line-derived EVs
- Fig. S3. Optimization of Isolation of HCC EV by Click Beads
- Fig. S4. Characterization of HepG2-derived EVs captured on Click Beads
- Fig. S5. Preparation of four TCO-conjugated HCC-specific antibodies
- Fig. S6. Conjugation of DNA barcode onto antibody and validation of the conjugated DNA-antibody
- Fig. S7. Workflow of HCC EV Surface Protein Assay for quantification of eight subpopulations of HCC EVs.
- Fig. S8. Expression of the four selected HCC-associated surface markers in EVs from HCC cells, immortalized human hepatocytes, and primary human hepatocytes
- Fig. S9. Optimization of HCC EV Surface Protein Assay using HCC cell line-derived EVs
- Fig. S10. Validation of reproducibility of HCC EV Surface Protein Assay using clinical plasma samples
- Fig. S11. ROC curve of the eight HCC EV subpopulations for detecting early-stage HCC from cirrhosis in the UCLA training cohort
- Fig. S12. Calibration plot of HCC EV ECG score
- Fig. S13. ROC curve of HCC EV ECG score, serum AFP, and the combination of HCC EV ECG score and AFP for detecting early-stage HCC from cirrhosis in the UCLA training cohort
- Fig. S14. Comparison of HCC EV ECG scores between HCC and other cancers
- Fig. S15. Association between HCC EV ECG score, serum AFP level, serum ALT level, and MELD score among early-stage HCC patients and cirrhosis patients
- Fig. S16. ROC curve of HCC EV ECG score for detecting early-stage HCC from cirrhosis in the subgroups by etiology

### **SUPPLEMENTARY TABLES**

- Table S1. The sequences of the two DNA barcodes and their corresponding primers/probes for the duplex real-time PCR
- Table S2. Intra-assay, inter-assay coefficients of variation, and the comparison between the internal controls of HCC EV Surface Protein Assay

- Table S3. The relative PCR readouts for evaluation of reproducibility of HCC EV Surface Protein Assay
- Table S4. Univariate logistic regression analysis of the eight HCC subpopulations for detecting early-stage HCC from cirrhosis
- Table S5. Confusion matrix for HCC EV ECG score in the UCLA training cohort ( $n=106$ )
- Table S6. Misclassification tables and NRI for evaluating the improvement by adding serum AFP level to HCC EV ECG score in the UCLA training cohort ( $n=102$ )
- Table S7. Demographic and clinical characteristics of the patients with other cancers
- Table S8. Confusion matrix for HCC EV ECG score in the CSMC validation cohort ( $n=72$ )
- Table S9. Confusion matrix for HCC EV ECG score and serum AFP among all the participants in this study ( $n=172$ )
- Table S10. Demographic and clinical characteristics of the cirrhotic cohort after frequency matching of the etiology ( $n=117$ )

## REFERENCES

## **SUPPLEMENTARY METHODS**

### **Testing the four HCC-associated surface protein markers in HCC tissue microarray (TMA)**

Hematoxylin and Eosin (H&E) and immunohistochemistry (IHC) staining of the four HCC-associated surface protein markers were performed in a 708-sample HCC TMA generated from archived, resected HCC specimens at the University of California, Los Angeles (UCLA). The HCC tissues were fixed in 10% neutral formalin for 24h and embedded in paraffin according to the standard operating procedure for tissue in the pathology department at UCLA. Serial 5 µm-thick tissue microarray slides from formalin-fixed paraffin-embedded blocks were cut and mounted on poly-L-lysine coated glass slides. Standard IHC staining was performed according to a protocol optimized for each antibody, including anti-EpCAM (Cell Signaling, Danvers, MA), anti-CD147 (R&D Systems, Minneapolis, MN), anti-glypican-3 (GPC3; Santa Cruz Biotechnology, Santa Cruz, CA), and anti-asialoglycoprotein receptor (ASGPR; Abcam, Cambridge, UK). All slides were scanned and converted to high resolution digital images with magnification of 40X using the Aperio ScanScope AT high throughput scanning system. The IHC staining results were evaluated using a four-point scale staining intensity (none, 0; weak, 1<sup>+</sup>; moderate, 2<sup>+</sup>; strong, 3<sup>+</sup>) on digital pathology slides by the pathologist (Y. Z.). The HCC tissues were considered to have stained positive if they displayed weak (1<sup>+</sup>), moderate (2<sup>+</sup>) or strong (3<sup>+</sup>) staining to the antibodies tested. The raw data of the 708-sample HCC TMA was provided in the Supplementary Excel Sheet.

### **Definition of etiologies of underlying liver disease**

HBV infection was confirmed by positive HBsAg. Hepatitis C virus (HCV) infection was confirmed by (i) HCV RNA or (ii) chronic liver disease with positive anti-HCV. Alcoholic liver disease (ALD) was confirmed by (i) a documented history of ALD or (ii) a significant history of alcohol abuse or alcohol addiction. Nonalcoholic fatty liver disease (NAFLD) was diagnosed

by (i) histologic or radiologic evidence of fatty infiltration or inflammation without any history of significant alcohol intake (<20 g per day), or (ii) clinical evidence suggesting risk factors for fatty liver disease such as metabolic syndrome without any history of significant alcohol intake.

### **Blood sample processing**

Peripheral venous blood samples were collected from participants with written informed consent according to the IRB protocols at UCLA and CSMC. A 10.0-mL ethylenediaminetetraacetic acid vacutainer tube (BD Medical, Fisher Cat. #BD 366643-1) was used for blood sample collection. The whole blood was centrifuged at 530 g for 10 min, and the supernatant was retrieved and centrifuged at 4,600 g for 10 min. The final supernatant was collected as plasma samples and stored in -80°C refrigerators. All the plasma samples were retrieved just before being subjected to HCC EV SPA.

### **Testing the four HCC-associated surface protein markers in HCC cell line-derived EVs using Western blot**

Western blot analysis was performed to quantify the four HCC-associated surface protein markers from the EVs. The collected HepG2-, Hep3B-, Huh-7-, MIHA-, and primary human hepatocyte-derived EVs were lysed in an appropriate volume of Radioimmunoprecipitation assay buffer on ice for 30 min followed by centrifugation at 14,000 g for 20 min. The protein concentration was assessed using Qubit assay (Thermo Fisher Scientific). The loading buffers (G-Biosciences) were added and the protein samples were then heated to 95 °C for 5 min. Protein samples were then separated on sodium dodecyl sulfate-polyacrylamide gel electrophoresis, then transferred to polyvinylidene fluoride membranes, blocked in 5% non-fat milk in TBS-T (containing 0.1% Tween-20) for 1 h. The membranes were first incubated with antibodies against  $\beta$ -actin (Sigma-Aldrich Chemie, Steinheim, Germany), EpCAM, CD147,

GPC3, and ASGPR1, overnight at 4 °C, respectively, and the primary antibodies above were dissolved in corresponding blocking solutions, then followed by 1 h incubation with the appropriate secondary antibody. The results were visualized using an enhanced chemiluminescence system.

### **Optimization and validation of Click Beads using HepG2-derived EVs**

To evaluate the performance of Click Beads for capturing HCC EVs, we prepared HCC cell line-derived EVs according to our previous protocol.<sup>1</sup> Characterization of HepG2-derived EVs (**Supplementary Figure 4**) was performed following the Minimal information for studies of extracellular vesicles (MISEV) 2018<sup>2</sup> and MISEV 2014<sup>3</sup> guidelines issued by the International Society for Extracellular Vesicles. The evaluation of Click Beads for capturing HCC EVs is summarized in **Supplementary Figure 5-6**.

### **Optimization and validation of HCC EV SPA using HepG2-derived EVs**

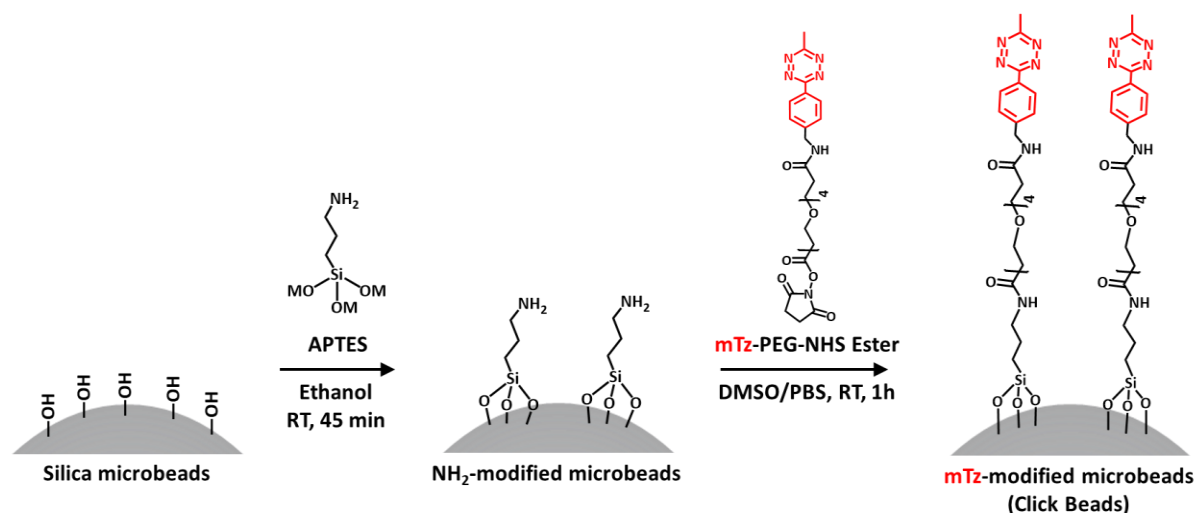
HepG2-derived EVs were used to optimize and validate HCC EV SPA (**Supplementary Figure 9**). We first blocked Click Beads with 5% BSA, Pierce™ Protein-Free (PBS) Blocking Buffer (PFBS, Thermofisher, #37572), respectively. Then, a DNA-control IgG (anti-PSA, monoclonal mouse IgG1, Abcam) conjugate and DNA-anti-CD63 was used to quantify the EpCAM<sup>+</sup> subpopulation of HepG2-derived EVs, respectively, to validate the efficacy of DNA-anti-CD63. For the dilution series, concentrations of 10<sup>4</sup>, 10<sup>5</sup> and 10<sup>6</sup> particles/μL were spiked into FBS for subpopulation EV isolation with TCO-anti-EpCAM, TCO-anti-ASGPR1, TCO-anti-GPC3 and TCO-anti-CD147, respectively, cocktailed with DNA-anti-CD63 at room temperature for 30 min. As an internal control, FBS samples without spiking HepG2-derived EVs were performed. The samples labeled with TCO-antibodies and DNA-anti-CD63 were then incubated with the EV Click Beads (0.1 mg) for 30 min for the subpopulation EV isolation. Click Beads with isolated EVs were collected by centrifuge at 10,000 g, 2 min. After 5-time

washing steps, Click Beads were measured as described above.

### **Evaluation of reproducibility of HCC EV SPA**

To test the general applicability of HCC EV SPA, the reproducibility of the HCC EV SPA was evaluated by calculating the percent coefficient of variation (%CV) relative signals. Technical triplicates of two plasma samples from patients with cirrhosis and two plasma samples from patients with HCC were processed with HCC EV SPA by the operators at different timepoints. The evaluation of reproducibility of HCC EV SPA is summarized in **Supplementary Figure 10** and **Supplementary Table 3**.

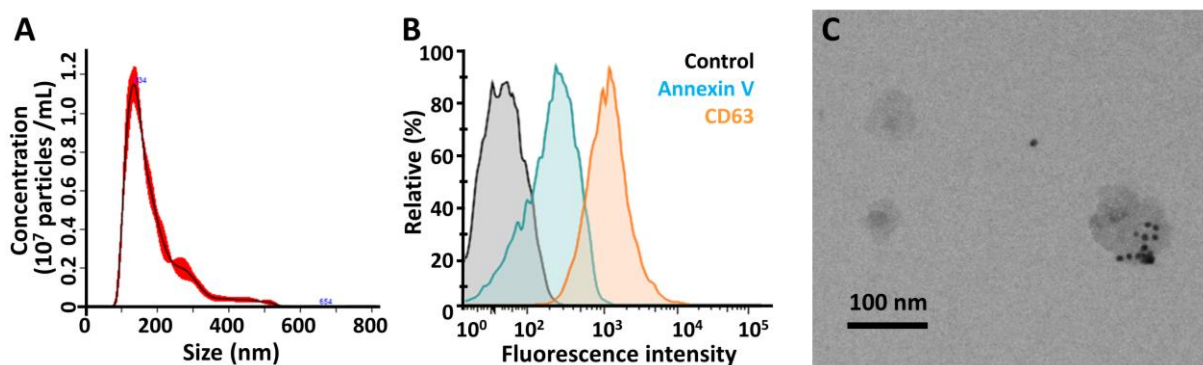
## SUPPLEMENTARY FIGURES



**Supplementary Figure 1. Fabrication<sup>4</sup> of Click Beads.** We prepared the Click Beads by designing a three-step chemical modification procedure: (i) The silica microbeads with natural hydroxyl (silica MBs, Bangs Laboratories, Inc) were first treated with nitric acid (2 mol/L, Sigma-Aldrich) for 30 min, followed by washing with DI water and ethanol successively. (ii) The resultant silica MBs were then resuspended in (3-aminopropyl) triethoxysilane/ethanol solution (4%, v/v, Sigma-Aldrich) for 45 min to introduce terminal amine groups. Then the amine-terminated silica microbeads (NH<sub>2</sub>-modified MBs) were washed with ethanol three times. (iii) To graft mTz motifs, the NH<sub>2</sub>-modified MBs was incubated with methyltetrazine-sulfo-NHS Ester (3.8 mM, Click Chemistry Tools) in PBS (200 μL, PH=8.5) for 1 h. The resulting mTz-grafted MBs were washed with DI water three times. After drying under nitrogen flow, the mTz-grafted MBs were stored at 4°C and retrieved just before use.

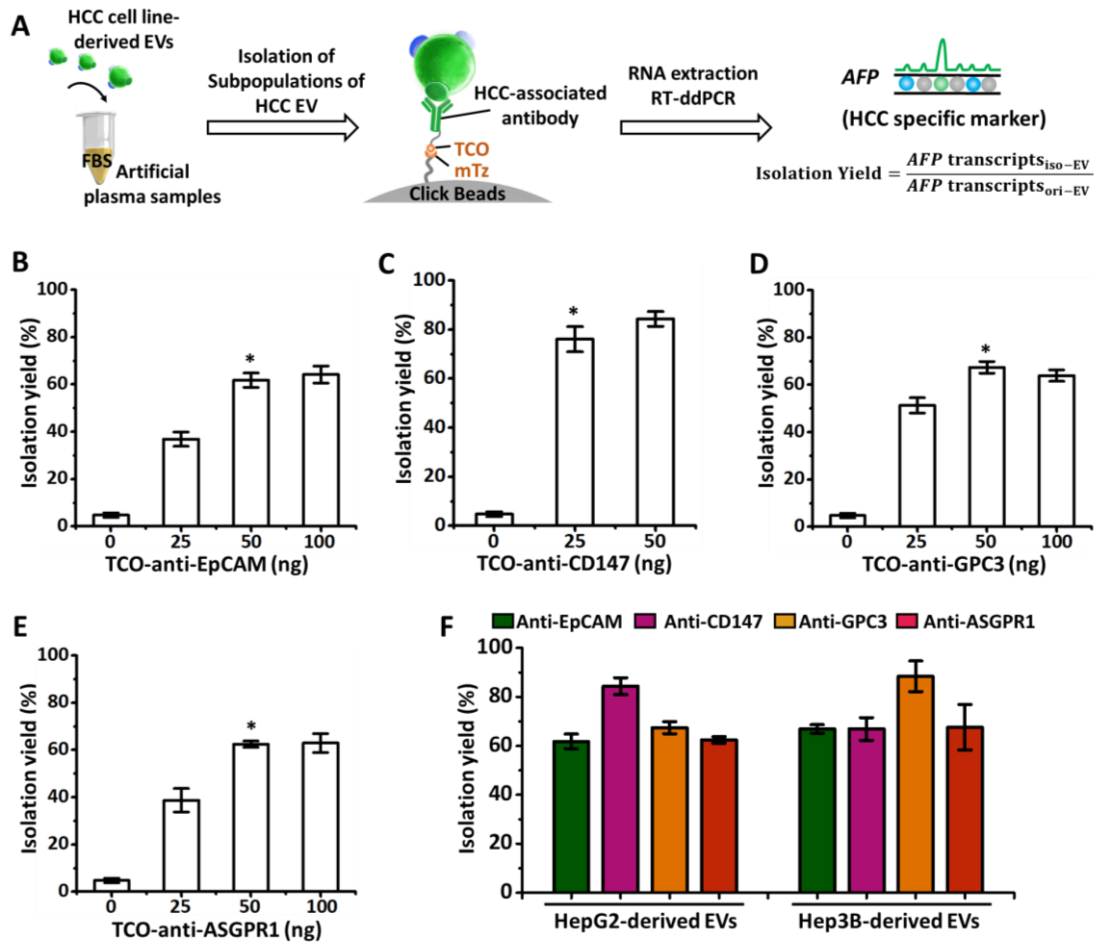
APTES, aminopropyltriethoxysilane; DI, deionization; DMSO, dimethyl sulfoxide; MBs, microbeads; mTz, methyltetrazine; NHS, N-hydroxylsuccinimide; PBS, phosphate-buffered saline; PEG, polyethylene glycol; RT, room temperature.





**Supplementary Figure 2. Characterization of HCC cell line-derived EVs.** HCC cell line-derived EVs were prepared according to our previous protocol.<sup>1</sup> Characterization of HepG2-derived EVs was performed following the MISEV 2018<sup>2</sup> and MISEV 2014<sup>3</sup> guidelines issued by the International Society for Extracellular Vesicles. **(A)** Concentration and size distributions of HepG2-derived EVs (diluted 1:100 in PBS) were measured by nanoparticle tracking analysis using a NanoSight NS300 (Malvern Instruments Ltd, Malvern, UK). The size of the HepG2-derived EVs ranges from 80 to 550 nm. **(B)** Expression of EV markers (CD63 and Annexin V) on HepG2-derived EVs was analyzed by flow cytometry. **(C)** Representative TEM image of HepG2-derived EVs in bulk solution before capture with immunogold labeling. EVs are identified and highlighted with gold nanoparticles via anti-CD63. Scale bar, 100 nm. In brief, fixed EVs in PBS were incubated with anti-CD63 (Abcam, mouse, 1:100 dilution) for 30 min. Then, these samples were incubated with nanogolds-conjugated anti-mouse IgG (12 nm, 1:50 dilution) for 1 h. These gold-labeled samples were dropped onto carbon coated copper grids and incubated for 10 min before being wiped off from the grids. After being rinsed 5 times using water, grids were dried for TEM imaging.

EV, extracellular vesicle; HCC, hepatocellular carcinoma; MISEV, Minimal information for studies of extracellular vesicles; mTz, methyltetrazine; TCO, trans-cyclooctene; TEM, transmission electron microscopy.



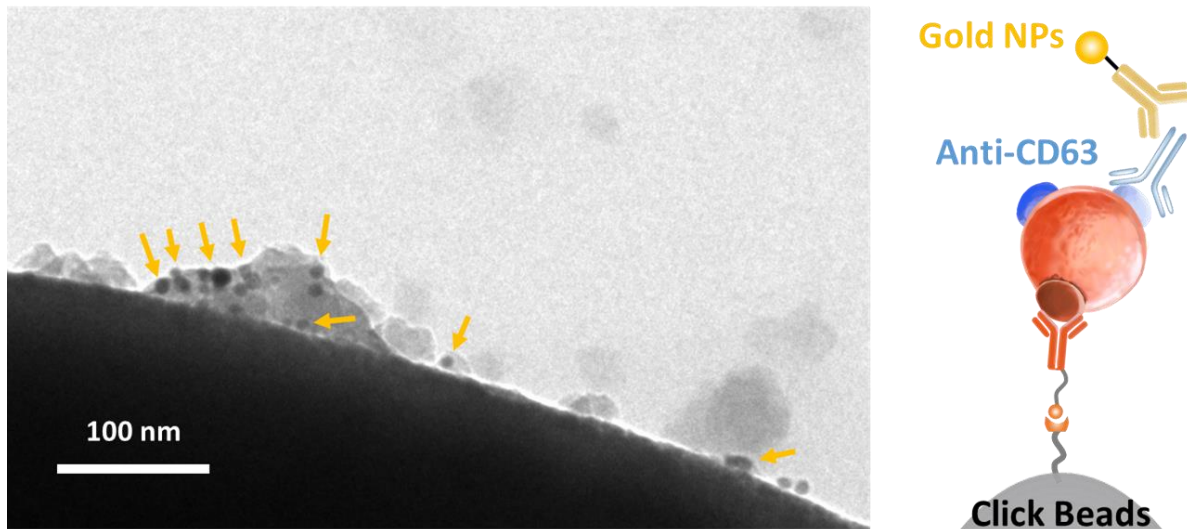
**Supplementary Figure 3. Optimization of Isolation of HCC EV by Click Beads<sup>4</sup>.** (A) A quantitative method for evaluating the isolation yield of HCC EV by Click Beads. Artificial plasma samples were prepared by spiking 10  $\mu\text{L}$  aliquot of HCC cell line-derived EV pellets into 90  $\mu\text{L}$  healthy donors' plasma. Since *AFP* transcript was absent in the healthy donor's plasma we tested, the isolation yield of HCC cell line-derived EVs by Click Beads can be calculated from the following equation using RT-ddPCR assay:

$$\text{EV isolation yield} = \frac{\text{AFP transcripts}_{\text{isolated}}}{\text{AFP transcripts}_{\text{original}}} \quad (1)$$

In brief, the original 10  $\mu\text{L}$  aliquot of HCC EVs and the isolated HCC EVs by Click Beads were lysed by 700  $\mu\text{L}$  QIAzol Lysis Reagent (Qiagen), respectively. RNA was extracted using a miRNeasy Micro Kit (Qiagen) following the manufacturer's instructions. The complementary DNA (cDNA) was synthesized using a Maxima H Minus Reverse

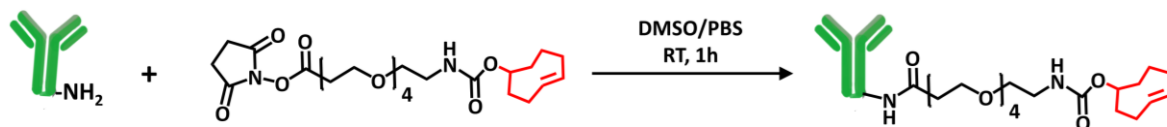
Transcriptase Kit (Thermo Scientific) following the manufacturer's instructions. cDNA was tested for *AFP* transcripts using duplex Droplet Digital PCR on a QX200 system (Bio-Rad Laboratories, Inc.) following the manufacturer's instructions and the resulting data were analyzed using the QuantaSoft™ software (Bio-Rad Laboratories, Inc.). The primer and probe for *AFP* were purchased from Thermo Fisher Scientific (*AFP*, Hs01040598\_m1, 4448489). **(B-E)** The isolation yields observed for Click Beads at different amounts of TCO-anti-EpCAM, TCO-anti-CD147, TCO-anti-GPC3, and TCO-anti-ASGPR1, respectively, using the artificial plasma samples spiked with HepG2-derived EVs. Data are presented as means  $\pm$  SD of three independent assays. Asterisks indicate the optimized amount of each TCO-conjugated antibody. **(F)** The isolation yields observed for Click Beads with the optimized amounts of TCO-conjugated antibodies using the artificial plasma samples spiked with HepG2-derived EVs and Hep3B-derived, respectively.

AFP, alpha-fetoprotein; ASGPR1, Asialoglycoprotein receptor 1; EpCAM, epithelial cellular adhesion molecule; EV, extracellular vesicle; GPC3, Glypican 3 Protein; HCC, hepatocellular carcinoma; iso, isolated; mTz, methyltetrazine; ori, original; RT-ddPCR, reverse-transcription droplet digital PCR; SD, standard deviation; TCO, trans-cyclooctene.



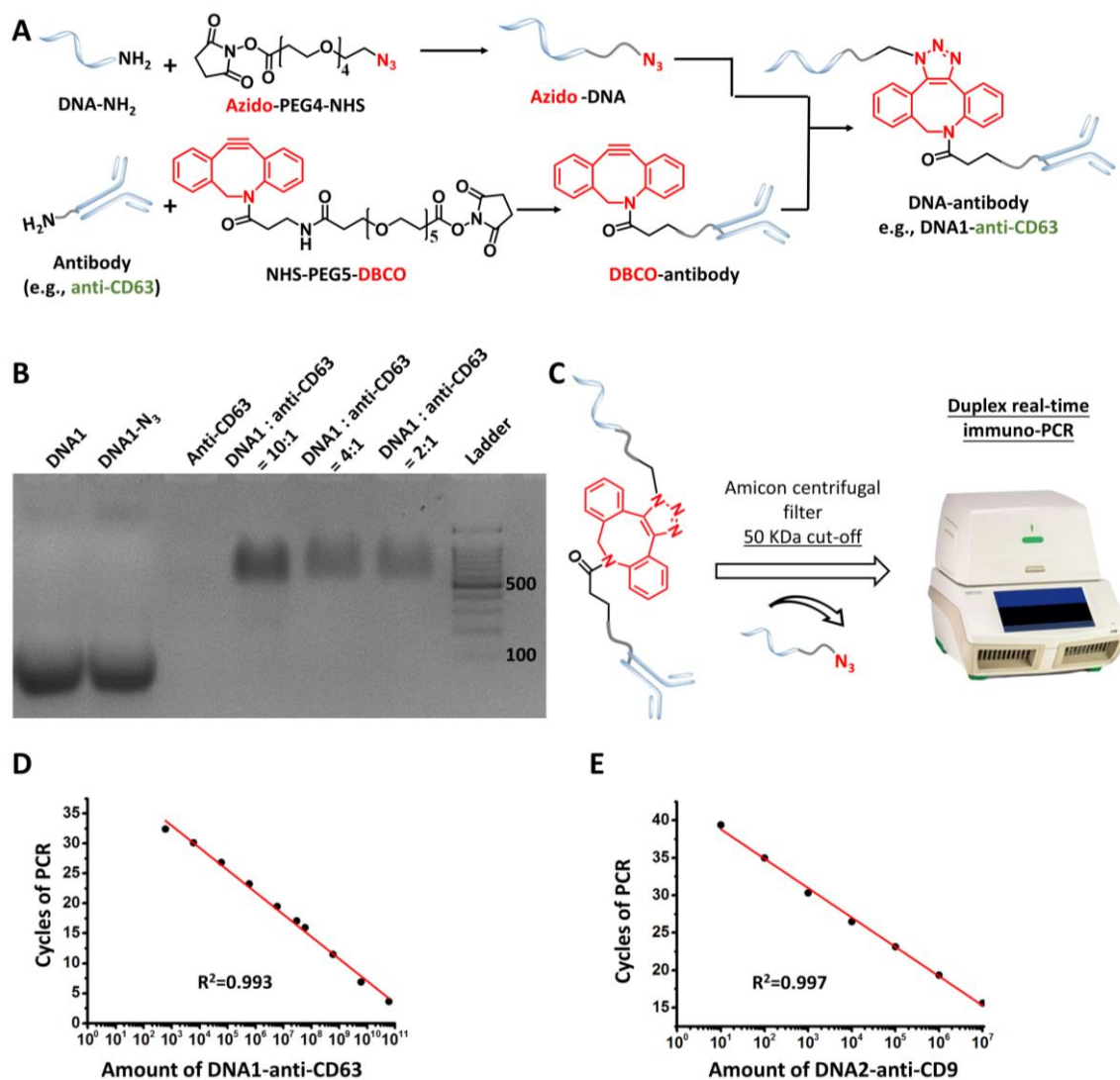
**Supplementary Figure 4. Characterization of HepG2-derived EVs captured on Click Beads.** Immunogold staining by anti-CD63 was employed in TEM imaging to verify the identity of HepG2-derived EVs captured on Click Beads. EVs are identified and highlighted with 12-nm gold nanoparticles via anti-CD63. Scale bar, 100 nm. Yellow arrows: gold nanoparticles.

EV, extracellular vesicle; HCC, hepatocellular carcinoma; NP, nanoparticle; TEM, transmission electron microscopy.



**Supplementary Figure 5. Preparation<sup>1</sup> of four TCO-conjugated HCC-specific antibodies.**

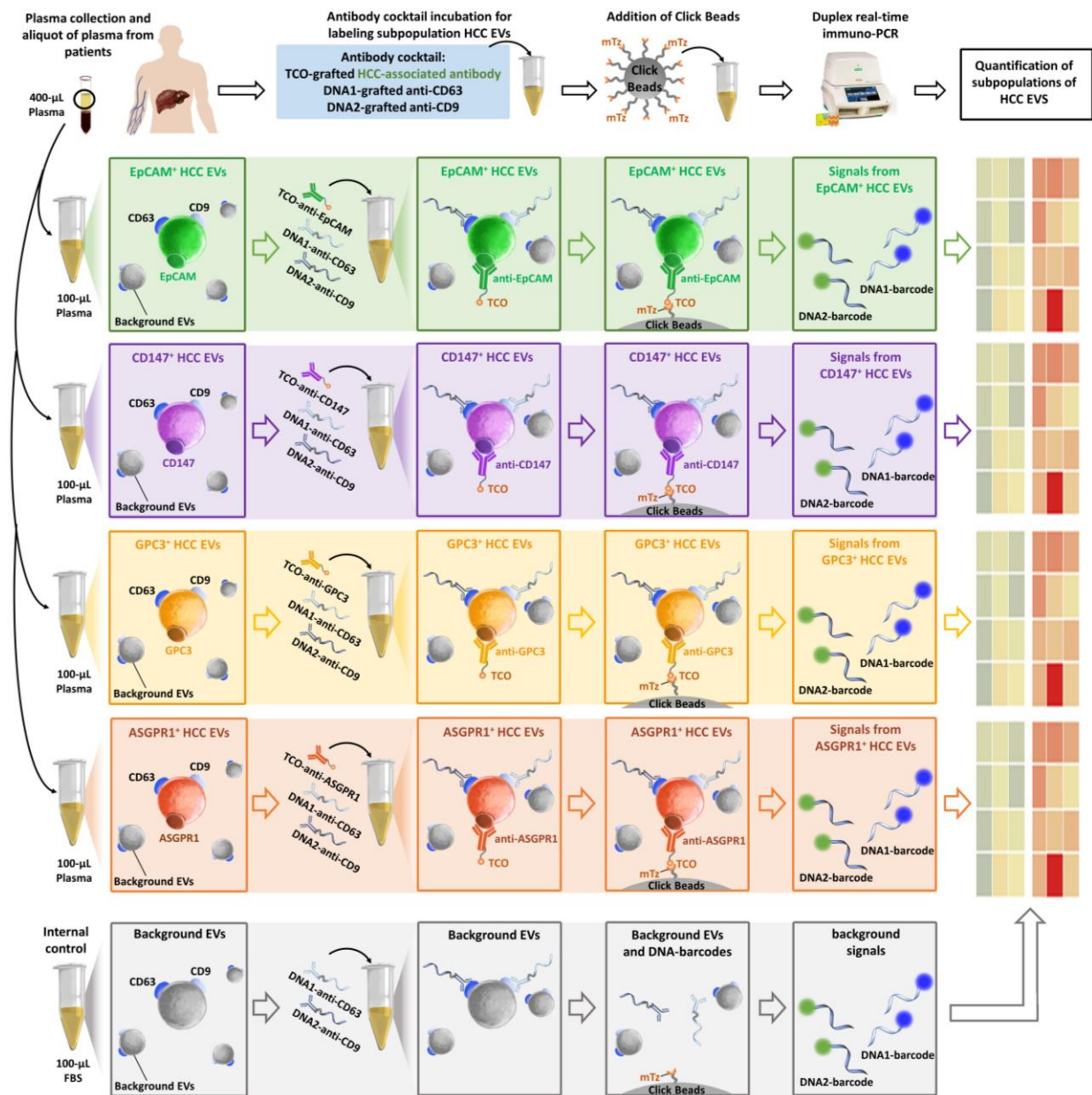
As we described in our previous publication,<sup>1</sup> goat anti-human EpCAM (R&D Systems, Inc., reconstitute at 0.2 mg/mL, dilute 200 to 2,000 times in samples), rabbit anti-human ASGPR1 (LifeSpan BioSciences, Inc., 1 mg/ml, dilute 1,000-10,000 times in samples), sheep anti-human GPC3 (R&D Systems, Inc., reconstitute at 0.2 mg/mL, dilute 200-2,000 times in samples), and goat anti-human CD147 (R&D Systems, Inc., reconstitute at 0.5 mg/mL, dilute 1,000-2,000 times in samples), were incubated with TCO-PEG<sub>4</sub>-NHS ester (0.5 mM, Click Chemistry Tools Bioconjugate Technology Company) in PBS at the mole ratio of 1:4, respectively, at room temperature for 30 min. The individual TCO-conjugated antibody was prepared just before use. ASGPR1, Asialoglycoprotein receptor 1; DMSO, dimethyl sulfoxide; EpCAM, epithelial cellular adhesion molecule; GPC3, Glypican 3 Protein; NHS, N-hydroxylsuccinimide; PBS, phosphate-buffered saline; PEG, polyethylene glycol; RT, room temperature; TCO, trans-cyclooctene.



**Supplementary Figure 6. Conjugation of DNA barcode onto antibody and validation of the conjugated DNA-antibody.** (A) Steps of conjugation of DNA barcodes onto antibodies for targeting EV markers, CD63 and CD9. (i) Production of N<sub>3</sub>-DNA: The DNA barcodes were purchased from IDT and the sequences are listed in **Supplementary Table 1**. N<sub>3</sub>-DNA was produced by incubating DNA barcodes with azido-PEG<sub>4</sub>-NHS (Click Chemistry Tools) in the molar ratio of 1:20 at room temperature for 4 h. Surplus azido-PEG<sub>4</sub>-NHS was removed using Amicon Ultra-0.5 Centrifugal Filter Unit (10K, Millipore). (ii) Preparation of DBCO-antibodies: For anti-CD63 AND anti-CD9, a buffer exchange was performed using 40K Zeba™ spin desalting columns (Thermo Scientific) to 50 mM borate buffered saline (BBS, pH 8.4). Antibodies were incubated for 45 min with NHS-PEG<sub>5</sub>-DBCO (Click Chemistry Tools)

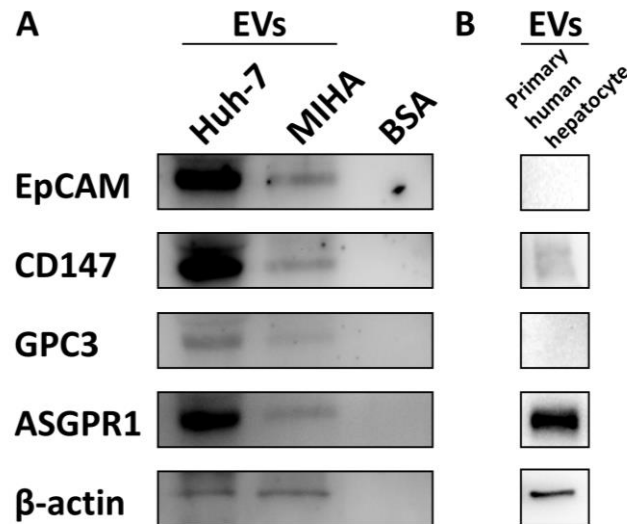
in the molar ratio of 1:10 at room temperature. Surplus NHS-PEG<sub>5</sub>-DBCO was removed using Amicon Ultra-0.5 Centrifugal Filter Unit (50K, Millipore). (iii) Conjugation of DNA-antibodies: SPAAC was used for functionalization of DBCO-antibodies with N<sub>3</sub>-DNA for overnight at 4°C. Conjugation of antibody and DNA was performed with a molar ratio of 1:2, 1:4 and 1:10 in PBS to determine functionalization efficiency. Surplus N<sub>3</sub>-DNA was removed using Amicon Ultra-0.5 Centrifugal Filter Unit (50 kDa, Millipore) for 2 times. DNA-antibodies were stored in a glycerin/PBS (1:1) solution at -20°C and retrieved just before use. **(B)** Gel electrophoresis was used to monitor the conjugation between the DNA-barcode and anti-CD63. Briefly, DNA, DNA-N<sub>3</sub> and DNA-antibody conjugates were run with DNA SafeStain (Lamda Biotech) on a 2% agarose gel (0.5 × TBE) and scanned on a gel documentation system. **(C)** After purification by Amicon centrifugal filter, DNA-conjugated EV-specific antibodies will be characterized by duplex real-time immune-PCR. The linearity of duplex real-time immuno-PCR for detecting **(D)** DNA1-anti-CD63,  $R^2=0.993$ , and **(E)** DNA2-anti-CD9,  $R^2=0.997$ , respectively.

DBCO, diarylcyclooctyne; EV, extracellular vesicle; IDT, Integrated DNA Technologies; NHS, N-Hydroxysuccinimide; PBS, phosphate buffered saline; PEG, polyethylene glycol; SPAAC, strain-promoted azide-alkyne cycloaddition.



**Supplementary Figure 7. Workflow of HCC EV Surface Protein Assay for quantification of eight subpopulations of HCC EVs.** HCC EV Surface Protein Assay is implemented through a 3-step workflow. Step 1: Sequentially labeling each subpopulation of HCC EVs in plasma. Step 2: Covalent Chemistry-mediated capture of subpopulations of HCC EVs onto Click Beads. Step 3: On-Bead duplex real-time immuno-PCR for quantifying each subpopulation of HCC EVs. ASGPR1, Asialoglycoprotein receptor 1; EpCAM, epithelial cellular adhesion molecule; EV, extracellular vesicle; GPC3, Glypican 3 Protein; HCC, hepatocellular carcinoma; mTz, methyltetrazine; TCO, trans-cyclooctene.

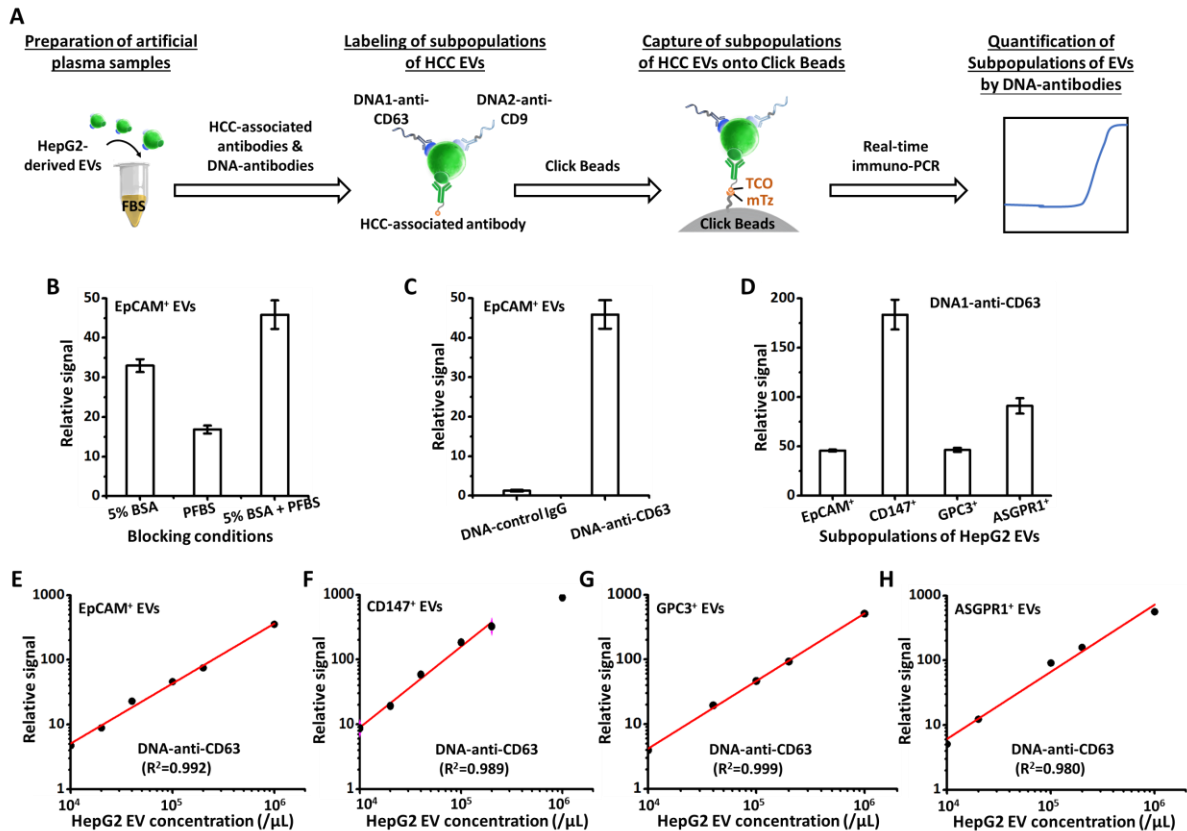




**Supplementary Figure 8. Expression of the four selected HCC-associated surface markers in EVs from HCC cells, immortalized human hepatocytes, and primary human hepatocytes. (A)** Western Blotting for the four surface protein markers, EpCAM, CD147, GPC3, and ASGPR1, in Huh7-derived EVs (HCC cell line-derived EVs) and MIHA-derived EVs (immortalized human hepatocyte cell line-derived EVs), with BSA as the negative control. **(B)** Western Blotting for the four surface protein markers in primary human hepatocyte-derived EVs.

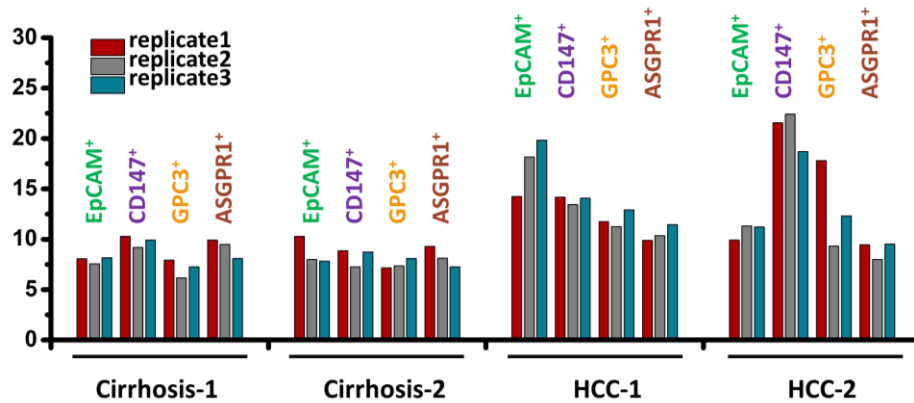
The human HCC cell line, Huh7, was purchased from ThermoFisher Scientific (Rockford, IL, USA). The immortalized human hepatocyte cell line, MIHA, was purchased from ATCC (Manassas, VA, USA). The primary human hepatocytes were obtained from Gibco™ HMCPIS (Grand Island, NY, USA). Huh7, MIHA, and primary human hepatocytes were cultured according to the manufacturers' instructions. EVs from the cell lines and cells were prepared according to our previous protocol.<sup>1</sup>

ASGPR1, asialoglycoprotein receptor 1; BSA, bovine serum albumin; EpCAM, epithelial cellular adhesion molecule; EV, extracellular vesicle; GPC3, glypican 3; HCC, hepatocellular carcinoma.

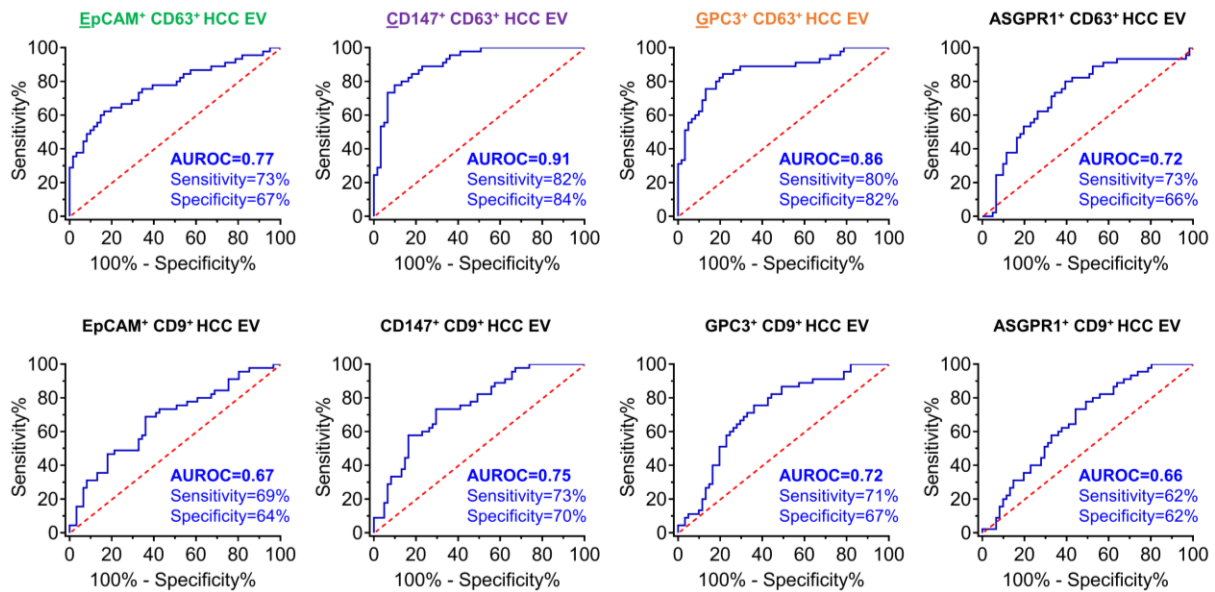


**Supplementary Figure 9. Optimization of HCC EV Surface Protein Assay using HCC cell line-derived EVs.** (A) The workflow of HCC EV Surface Protein Assay for quantitative detection of four subpopulations of HCC EVs (EpCAM<sup>+</sup> HCC EVs as an example) using artificial plasma samples, prepared by spiking 10<sup>7</sup> HepG2-derived EVs into 100 μL fetal bovine serum (FBS). A duplex real-time immuno-PCR was employed to quantify the copy numbers of DNA1-anti-CD63 labelled on the purified subpopulations of EV samples. (B) Comparison of the relative signals from HCC EV Surface Protein Assay between different blocking conditions. 5% BSA combined with PFBS achieved the best blocking result. (C) DNA1-anti-CD63 has higher signals from HCC EV Surface Protein Assay compared with DNA-control IgG. (D) The relative signal of HCC EV Surface Protein Assay for detecting four subpopulations of HCC EVs. The highest signals were detected in CD147<sup>+</sup> subpopulations. Good linearity of HCC EV Surface Protein Assay for detecting HepG2 cells-derived EVs were achieved for (E) EpCAM<sup>+</sup> subpopulation, R<sup>2</sup>= 0.992; (F) CD147<sup>+</sup> subpopulation, R<sup>2</sup>= 0.989; (G) GPC3<sup>+</sup> subpopulation, R<sup>2</sup>= 0.999; and (H) ASGPR1<sup>+</sup> subpopulation, R<sup>2</sup>= 0.980, by DNA1-anti-CD63.

ASGPR1, Asialoglycoprotein receptor 1; EpCAM, epithelial cellular adhesion molecule; EV, extracellular vesicle; GPC3, Glypican 3 Protein; HCC, hepatocellular carcinoma; mTz, methyltetrazine; TCO, trans-cyclooctene.

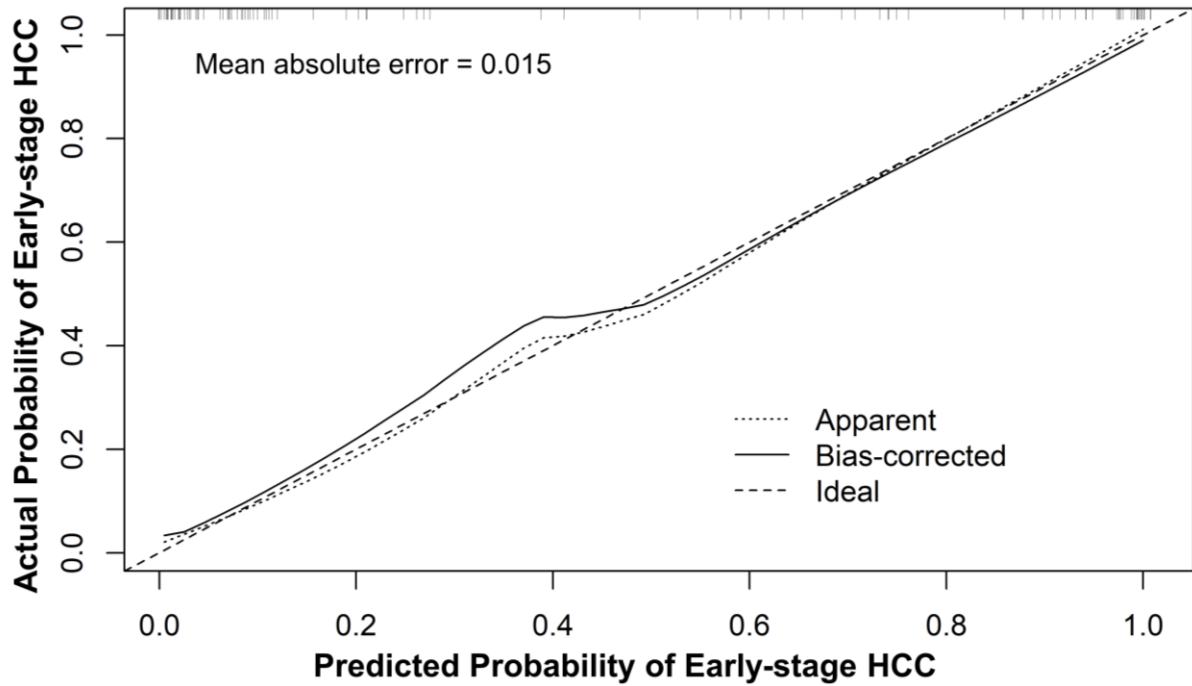


**Supplementary Figure 10. Validation of reproducibility of HCC EV Surface Protein Assay using clinical plasma samples.** Reproducibility of the quantification of the four HCC EV subpopulations (EpCAM<sup>+</sup> CD63<sup>+</sup> HCC EVs, CD147<sup>+</sup> CD63<sup>+</sup> HCC EVs, GPC3<sup>+</sup> CD63<sup>+</sup> HCC EVs, ASGPR1<sup>+</sup>CD63<sup>+</sup> HCC EVs) isolated from technical triplicate plasma samples from two patients with early-stage HCC and two patients with liver cirrhosis. The Coefficients of Variability (CV%) of each subpopulation for each sample is listed in Supplementary Table 2. ASGPR1, Asialoglycoprotein receptor 1; EpCAM, epithelial cellular adhesion molecule; EV, extracellular vesicle; GPC3, Glypican 3 Protein; HCC, hepatocellular carcinoma.

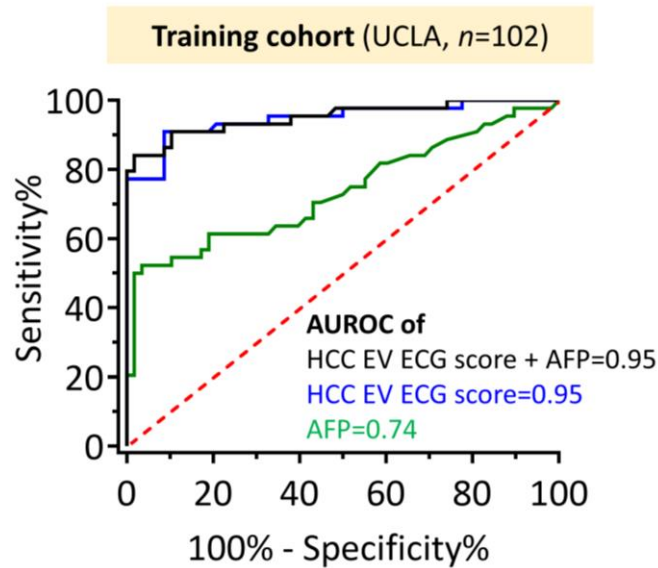


**Supplementary Figure 11. ROC curve of the eight HCC EV subpopulations for detecting early-stage HCC from cirrhosis in the UCLA training cohort.** ROC curves of EpCAM<sup>+</sup> CD63<sup>+</sup> HCC EVs, CD147<sup>+</sup> CD63<sup>+</sup> HCC EVs, GPC3<sup>+</sup> CD63<sup>+</sup> HCC EVs, ASGPR1<sup>+</sup> CD63<sup>+</sup> HCC EVs, EpCAM<sup>+</sup> CD9<sup>+</sup> HCC EVs, CD147<sup>+</sup> CD9<sup>+</sup> HCC EVs, GPC3<sup>+</sup> CD9<sup>+</sup> HCC EVs, and ASGPR1<sup>+</sup> CD9<sup>+</sup> HCC EVs, respectively, for distinguishing early-stage HCC from cirrhosis in the UCLA training cohort.

ASGPR1, asialoglycoprotein receptor 1; AUROC, area under the receiver operating characteristic; CI, confidence interval; EpCAM, epithelial cellular adhesion molecule; EV, extracellular vesicle; GPC3, glypican 3; HCC, hepatocellular carcinoma; ROC, receiver operating characteristic; UCLA, University of California, Los Angeles.

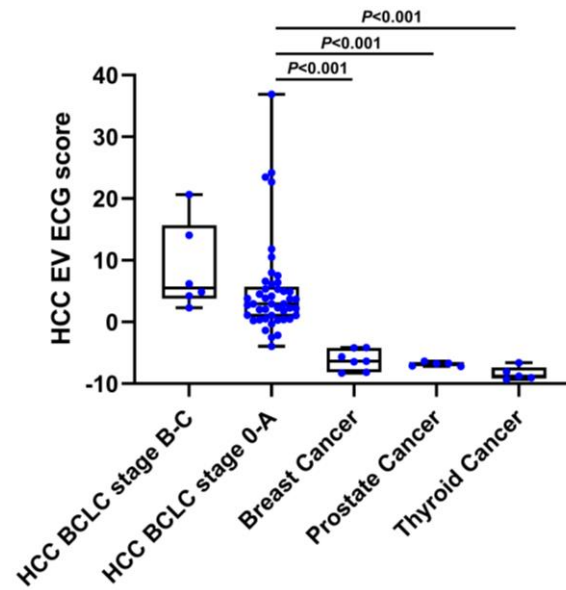


**Supplementary Figure 12. Calibration plot of HCC EV ECG score.** The apparent calibration curve was performed with the UCLA training cohort of 106 patients with HCC or cirrhosis. The bias-corrected calibration curve was generated by using 1,000 bootstrap resampling of the 106 patients. The predicted probability of early-stage HCC by HCC EV ECG score conforms well to the actual probability with a low mean absolute probability error (0.015). EV, extracellular vesicle; HCC, hepatocellular carcinoma; UCLA, University of California, Los Angeles.



**Supplementary Figure 13. ROC curve of HCC EV ECG score, serum AFP, and the combination of HCC EV ECG score and AFP for detecting early-stage HCC from cirrhosis in the UCLA training cohort.** Addition of serum AFP to HCC EV ECG score did not improve the performance for distinguishing early-stage HCC from cirrhosis in the UCLA training cohort (AUROC = 0.95 [95% CI = 0.91-1.00] vs. 0.95 [95% CI = 0.90-0.99],  $P=0.31$ , DeLong's test).

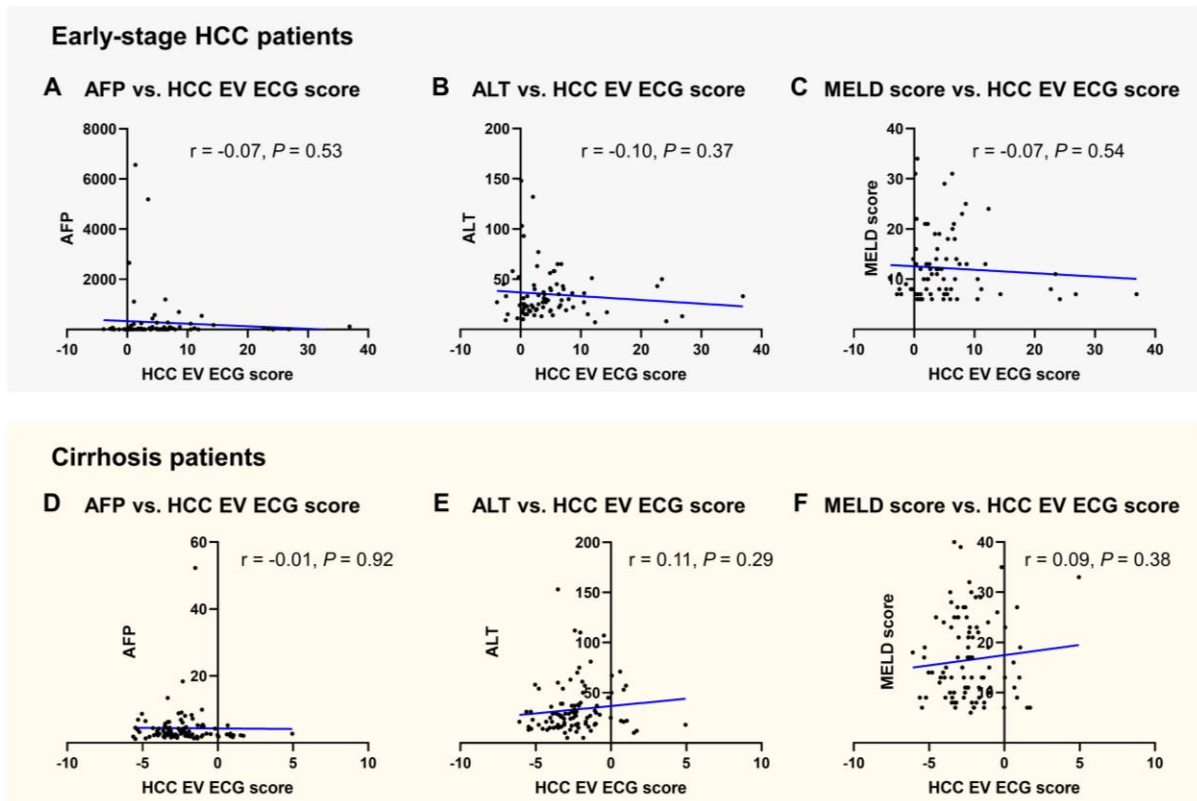
AFP, alpha-fetoprotein; AUROC, area under the receiver operating characteristic; CI, confidence interval; EV, extracellular vesicle; HCC, hepatocellular carcinoma; ROC, receiver operating characteristic; UCLA, University of California, Los Angeles.



**Supplementary Figure 14. Comparison of HCC EV ECG scores between HCC and other cancers.** The box plot summarized the HCC EV ECG scores from patients with BCLC stage 0-A HCC ( $n=45$ ), patients with BCLC stage B-C HCC ( $n=6$ ), patients with breast cancer ( $n=7$ ), patients with prostate cancer ( $n=5$ ), and patients with thyroid cancer ( $n=5$ ).

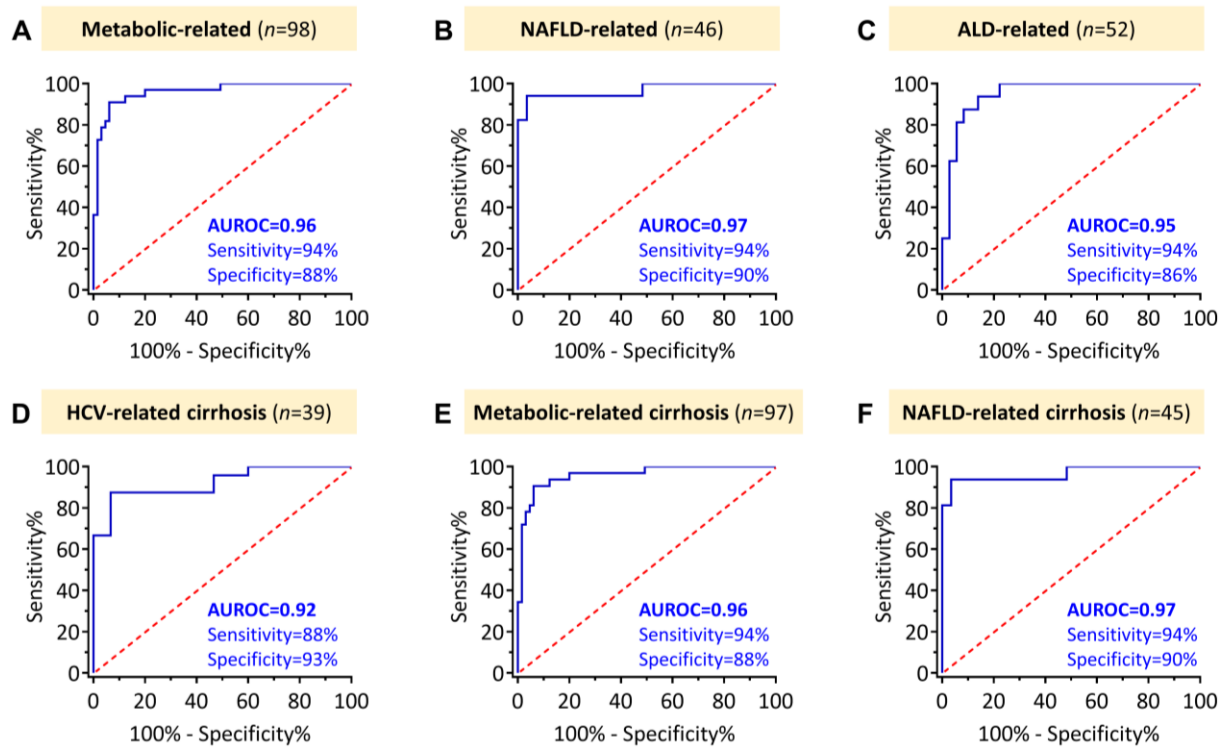
BCLC, Barcelona clinic liver cancer; EV, extracellular vesicle; HCC, hepatocellular carcinoma.





**Supplementary Figure 15. Association between HCC EV ECG score, serum AFP level, serum ALT level, and MELD score among early-stage HCC patients and cirrhosis patients. (A)** The association between serum AFP level and HCC EV ECG score among early-stage HCC patients. **(B)** The association between serum ALT level and HCC EV ECG score among early-stage HCC patients. **(C)** The association between MELD score and HCC EV ECG score among early-stage HCC patients. **(D)** The association between serum AFP level and HCC EV ECG score among cirrhosis patients. **(E)** The association between serum ALT level and HCC EV ECG score among cirrhosis patients. **(F)** The association between MELD score and HCC EV ECG score among cirrhosis patients. Each dot represents a patient.

AFP, alpha-fetoprotein; ALT, alanine transaminase; EV, extracellular vesicle; HCC, hepatocellular carcinoma; MELD, Model for End-stage Liver Disease.



**Supplementary Figure 16. ROC curve of HCC EV ECG score for detecting early-stage HCC from cirrhosis in the subgroups by etiology\*.** (A) ROC curve of HCC EV ECG score for detecting early-stage HCC from cirrhosis among patients with metabolic-related (NAFLD-related and ALD-related) etiology. (B) ROC curve of HCC EV ECG score for detecting early-stage HCC from cirrhosis among patients with NAFLD-related etiology. (C) ROC curve of HCC EV ECG score for detecting early-stage HCC from cirrhosis among patients with ALD-related etiology. (D) ROC curve of HCC EV ECG score for detecting early-stage HCC from cirrhosis among patients with HCV-related cirrhosis. (E) ROC curve of HCC EV ECG score for detecting early-stage HCC from cirrhosis among patients with metabolic-related (NAFLD-related and ALD-related) cirrhosis. (F) ROC curve of HCC EV ECG score for detecting early-stage HCC from cirrhosis among patients with NAFLD-related cirrhosis. The sensitivity and specificity were reported at the identified cutoff of -0.40.

\*Note: (i) the number of patients with HBV-related cirrhosis was too small to be analyzed;  
(ii) all the ALD-related patients were cirrhosis.

ALD, alcoholic liver disease; AUROC, area under the receiver operating characteristic; EV, extracellular vesicle; HBV, hepatitis B virus; HCC, hepatocellular carcinoma; HCV, hepatitis C virus; NAFLD, nonalcoholic fatty liver disease; ROC, receiver operating characteristic.

## SUPPLEMENTARY TABLES

**Supplementary Table 1. The sequences of the two DNA barcodes and their corresponding primers/probes for the duplex real-time PCR.**

DNA Barcode sequences		Primer/probe sequence	
<b>Barcode DNA 1 (for CD63)</b>	CGAGGGAAGTCTGATACAGCGGCAAGG ATCACGTTAGGCCGATGTGCCAATACGC CGACAATTGCCATACCGTCGTCCTCACTGC TT	<b>Forward</b>	AAGTCTGATACAGC GGCAAG
		<b>Reverse</b>	GCAGTGGACGACGG TATG
		<b>Probe (FAM)</b>	TCACGTTAGGCCGAT GTGCCAATA
<b>Barcode DNA 2 (for CD9)</b>	TGGTCTGTGGTGCTGTATTGAGCGGTGC GATCACGACATCACGACATCACGACCCA AACTGAGTAGCCTTCCC	<b>Forward</b>	TGGTCTGTGGTGCTG TATTG
		<b>Reverse</b>	GGGAAGGCTACTCA GTTTGG
		<b>Probe (HEX)</b>	TGCGATCACGACATC ACGACATCA

**Supplementary Table 2. Intra-assay, inter-assay coefficients of variation, and the comparison between the internal controls of HCC EV Surface Protein Assay.**

Run Number	FBS, Cq value					EV-depleted HD plasma, Cq value					P value
	Test 1	Test 2	Test 3	Mean	Intra CV (%)	Test 1	Test 2	Test 3	Mean	Intra CV (%)	
1	21.17	20.79	21.15	21.04	0.83	21.16	20.01	21.77	20.98	3.47	>0.99
2	20.77	22.43	21.97	21.73	3.22	22.20	20.75	22.52	21.82	3.53	>0.99
3	20.98	21.23	21.44	21.22	0.88	21.76	20.57	21.42	21.25	2.37	>0.99
4	21.34	21.59	21.57	21.50	0.53	21.00	20.59	21.34	20.98	1.45	0.10
5	22.17	21.72	21.48	21.79	1.30	20.79	20.84	20.49	20.71	0.75	0.10
	Inter CV (%)		1.35			Inter CV (%)		1.79			

To provide the justification of using FBS as an internal control of HCC EV Surface Protein Assay, we compared the signals between FBS and EV-depleted plasma samples from a healthy donor. In addition, intra-assay and inter-assay variability were measured to confirm the stability of the internal controls. Intra-assay variability was measured for one operator who performed three tests on one day, whereas inter-assay variability was measured across two operators who performed five runs total (one run per day), with each run consisting of three tests (15 tests total). The Cq values of FBS and EV-depleted plasma samples were consistent between each test and run with small coefficients of variation. Besides, the Cq values were comparable between FBS and EV-depleted plasma samples (Mann-Whitney *U* test,  $P > 0.005$ ), suggesting the feasibility of using FBS as an internal control for HCC EV Surface Protein Assay.

Cq, quantification cycle; CV, coefficient of variation; EV, extracellular vesicle; FBS, fetal bovine serum; HCC, hepatocellular carcinoma; HD, healthy donor; inter CV, inter-assay coefficient of variation; intra CV, intra-assay coefficient of variation.

**Supplementary Table 3. The relative signal for evaluation of reproducibility of HCC EV****Surface Protein Assay.**

<b>Patient</b>	<b>HCC EV subpopulation</b>	<b>Operator 1</b>	<b>Operator 2</b>	<b>Operator 3</b>	<b>%CV</b>
Cirrhosis-1	EpCAM <sup>+</sup> CD63 <sup>+</sup> HCC EVs	8.06	7.57	8.15	3.94
	CD147 <sup>+</sup> CD63 <sup>+</sup> HCC EVs	10.29	9.20	9.93	5.66
	GPC3 <sup>+</sup> CD63 <sup>+</sup> HCC EVs	7.92	6.17	7.24	12.41
	ASGPR1 <sup>+</sup> CD63 <sup>+</sup> HCC EVs	9.92	9.49	8.09	10.44
Cirrhosis-2	EpCAM <sup>+</sup> CD63 <sup>+</sup> HCC EVs	10.30	7.99	7.84	15.83
	CD147 <sup>+</sup> CD63 <sup>+</sup> HCC EVs	8.84	7.27	8.73	10.58
	GPC3 <sup>+</sup> CD63 <sup>+</sup> HCC EVs	7.16	7.35	8.08	6.45
	ASGPR1 <sup>+</sup> CD63 <sup>+</sup> HCC EVs	9.30	8.12	7.27	12.39
HCC-1	EpCAM <sup>+</sup> CD63 <sup>+</sup> HCC EVs	14.22	18.15	19.83	16.55
	CD147 <sup>+</sup> CD63 <sup>+</sup> HCC EVs	14.18	13.43	14.08	2.93
	GPC3 <sup>+</sup> CD63 <sup>+</sup> HCC EVs	11.74	11.25	12.92	7.17
	ASGPR1 <sup>+</sup> CD63 <sup>+</sup> HCC EVs	9.89	10.37	11.46	7.61
HCC-2	EpCAM <sup>+</sup> CD63 <sup>+</sup> HCC EVs	9.92	11.31	11.22	7.19
	CD147 <sup>+</sup> CD63 <sup>+</sup> HCC EVs	21.55	22.40	18.67	9.37
	GPC3 <sup>+</sup> CD63 <sup>+</sup> HCC EVs	17.81	18.66	12.32	21.16
	ASGPR1 <sup>+</sup> CD63 <sup>+</sup> HCC EVs	9.46	8.00	9.53	9.60

ASGPR1, asialoglycoprotein receptor 1; CV, coefficient of variation; EpCAM, epithelial cellular adhesion molecule; EV, extracellular vesicle; GPC3, glypican 3; HCC, hepatocellular carcinoma.

**Supplementary Table 4. Univariate logistic regression analysis of the eight HCC subpopulations for detecting early-stage HCC from cirrhosis.**

<b>EV subpopulation</b>	<b>Odds ratio</b>	<b>95% CI</b>	<b>P value</b>
EpCAM <sup>+</sup> CD63 <sup>+</sup> HCC EV	1.34	1.16-1.54	<0.001
CD147 <sup>+</sup> CD63 <sup>+</sup> HCC EV	1.56	1.32-1.84	<0.001
GPC3 <sup>+</sup> CD63 <sup>+</sup> HCC EV	1.58	1.31-1.89	<0.001
ASGPR1 <sup>+</sup> CD63 <sup>+</sup> HCC EV	1.10	1.02-1.19	0.01
EpCAM <sup>+</sup> CD9 <sup>+</sup> HCC EV	1.10	0.99-1.22	0.07
CD147 <sup>+</sup> CD9 <sup>+</sup> HCC EV	1.11	1.01-1.22	0.02
GPC3 <sup>+</sup> CD9 <sup>+</sup> HCC EV	1.14	1.03-1.25	0.009
ASGPR1 <sup>+</sup> CD9 <sup>+</sup> HCC EV	1.06	0.97-1.16	0.16

ASGPR1, asialoglycoprotein receptor 1; CI, confidence interval; EpCAM, epithelial cellular adhesion molecule; EV, extracellular vesicle; GPC3, glypican 3; HCC, hepatocellular carcinoma.

**Supplementary Table 5. Confusion matrix for HCC EV ECG score in the UCLA training cohort ( $n=106$ ).**

-	<b>HCC EV ECG (cutoff = -0.40)</b>		-
<b>Actual</b>	Predicted HCC	Predicted non-HCC	-
HCC	41	4	Sensitivity=91%
Cirrhosis	6	55	Specificity=90%
-	PPV=87%	NPV=93%	Accuracy=91%

EV, extracellular vesicle; HCC, hepatocellular carcinoma; NPV, negative predictive value; PPV, positive predictive value; UCLA, University of California, Los Angeles.



**Supplementary Table 6. Misclassification tables and NRI for evaluating the improvement by adding serum AFP level to HCC EV ECG score in the UCLA training cohort (\* $n=102$ ).**

**Cases (HCC,  $n = 44$ )**

Probability	HCC EV ECG score + AFP	
<b>HCC EV ECG score</b>	< 0.5 (False negative)	$\geq$ 0.5 (True positive)
< 0.5 (False negative)	4 (9.1%)	0 (0%)
$\geq$ 0.5 (True positive)	2 (4.5%)	38 (86.4%)

**Controls (Cirrhosis,  $n = 58$ )**

Probability	HCC EV ECG score + AFP	
<b>HCC EV ECG score</b>	< 0.5 (True negative)	$\geq$ 0.5 (False positive)
< 0.5 (True negative)	52 (89.7%)	1 (1.7%)
$\geq$ 0.5 (False positive)	0 (0%)	5 (8.6%)

$NRI^{all} = -0.06$  (95% CI = -0.06 to 0.16)

$NRI^{case} = -0.05$  (95% CI = -0.07 to 0.08)

$NRI^{control} = -0.02$  (95% CI = -0.02 to 0.11)

\*Individuals without serum AFP records ( $n = 4$ ) were excluded from the analysis.

AFP, alpha-fetoprotein; EV, extracellular vesicle; HCC, hepatocellular carcinoma; NRI, net reclassification improvement index; UCLA, University of California, Los Angeles.

**Supplementary Table 7. Demographic and clinical characteristics of the patients with other cancers.**

<b>Characteristic</b>	<b>BCLC stage B-C HCC (n=6)</b>	<b>Breast Cancer (n=7)</b>	<b>Prostate Cancer (n=5)</b>	<b>Thyroid Cancer (n=5)</b>
Age, y (IQR)	69 (64-74)	60 (51-67)	71 (58-79)	48 (45-72)
Gender, n (%)	-	-	-	-
Female	3 (50%)	7 (100%)	0 (0%)	2 (40%)
Male	3 (50%)	0 (0%)	5 (100%)	3 (60%)
Race/ethnicity, n (%)	-	-	-	-
White	2 (33.3%)	3 (42.9%)	4 (80%)	2 (40%)
Black	0 (0%)	0 (0%)	1 (20%)	0 (0%)
Asian	3 (50%)	1 (14.3%)	0 (0%)	2 (40%)
Hispanic	1 (16.7%)	2 (28.6%)	0 (0%)	1 (20%)
Others/Unknown	0 (0%)	1 (14.3%)	0 (0%)	0 (0%)
Tumor stage, n (%)	-	-	-	-
AJCC stage 0	0 (0%)	2 (28.6%)	0 (0%)	0 (0%)
AJCC stage I	0 (0%)	5 (71.4%)	3 (60%)	3 (60%)
AJCC stage II	5 (83.3%)	0 (0%)	1 (20%)	2 (40%)
AJCC stage III	1 (16.7%)	0 (0%)	1 (20%)	0 (0%)

AJCC, American Joint Committee on Cancer; BCLC, Barcelona clinic liver cancer; HCC, hepatocellular carcinoma; IQR, interquartile range.

**Supplementary Table 8. Confusion matrix for HCC EV ECG score in the CSMC validation cohort ( $n=72$ ).**

-	<b>HCC EV ECG (cutoff = -0.40)</b>		-
<b>Actual</b>	Predicted HCC	Predicted non-HCC	-
HCC	32	3	Sensitivity=91%
Cirrhosis	7	30	Specificity=81%
-	PPV=82%	NPV=91%	Accuracy=86%

CSMC, Cedars-Sinai Medical Center; EV, extracellular vesicle; HCC, hepatocellular carcinoma; NPV, negative predictive value; PPV, positive predictive value.

**Supplementary Table 9. Confusion matrix for HCC EV ECG score and serum AFP among all the participants in this study (\* $n=172$ ).**

-	<b>HCC EV ECG (cutoff = -0.40)</b>		-
<b>Actual</b>	Predicted HCC	Predicted non-HCC	-
HCC	71	7	Sensitivity=91%
Cirrhosis	13	81	Specificity=86%
-	PPV=85%	NPV=92%	Accuracy=88%

-	<b>Serum AFP (cutoff = 20 ng/mL)</b>		-
<b>Actual</b>	Predicted HCC	Predicted non-HCC	-
HCC	35	43	Sensitivity=45%
Cirrhosis	1	93	Specificity=99%
-	PPV=97%	NPV=68%	Accuracy=74%

\*Individuals without serum AFP records ( $n = 6$ ) were excluded from the analyses.

AFP, alpha-fetoprotein; EV, extracellular vesicle; HCC, hepatocellular carcinoma; NPV, negative predictive value; PPV, positive predictive value.

**Supplementary Table 10. Demographic and clinical characteristics of the cirrhotic cohort after frequency matching of the etiology (n=117).**

<b>Cirrhotic cohort after frequency matching of the etiology (n = 117)</b>			
Characteristic	Early-stage HCC (n=51)	Cirrhosis (n=66)	P value
Age, y (IQR)	64 (59-68)	61 (54-68)	0.11
Gender, n (%)	-	-	0.06
Female	15 (29.4)	32 (48.5)	-
Male	36 (70.6)	34 (51.5)	-
Race/ethnicity, n (%)	-	-	0.25
White	17 (33.3)	21 (31.8)	-
Black	2 (3.9)	1 (1.5)	-
Asian	6 (11.8)	12 (18.2)	-
Hispanic	25 (49.0)	25 (37.9)	-
Others/Unknown	1 (2.0)	7 (10.6)	-
Child-Pugh Score, n (%)	-	-	0.09
A	31 (60.8)	29 (43.9)	-
B-C	20 (39.2)	37 (56.1)	-
MELD score (IQR)	12 (8-16)	13 (9-18)	0.45
Etiology, n (%)	-	-	0.76
HBV	4 (7.8)	5 (7.5)	-
HCV	17 (33.3)	15 (22.7)	-
ALD	15 (29.4)	25 (37.9)	-
NAFLD	11 (22.6)	16 (24.2)	-
Others	4 (8.8)	5 (7.6)	-
Cirrhosis, n (%)	51 (100.0)	66 (100.0)	1.00
ALT, median (IQR)	30 (19-45)	25.5 (17.8-37)	0.26
AFP, median (IQR)	10.4 (3.9-54.7)	3 (2.3-4.7)	<0.001
AFP <20, n (%)	29 (56.8)	62 (94.0)	-
AFP ≥20, n (%)	21 (41.2)	1 (1.5)	-
NA, n (%)	1 (2.0)	3 (4.5)	-
Tumor stage	-	-	-
Very early (BCLC 0), n (%)	13 (25.5)	NA	-
Early (BCLC A), n (%)	38 (74.5)	NA	-
Single tumor, n (%)	47 (92.1)	NA	-
Largest tumor, cm (IQR)	2.6 (2-3.8)	NA	-
Within Milan criteria, n (%)	46 (90.2)	NA	-

AFP, alpha-fetoprotein; ALD, alcoholic liver disease; ALT, alanine aminotransferase; BCLC, Barcelona clinic liver cancer; HBV, hepatitis B virus; HCC, hepatocellular carcinoma; HCV, hepatitis C virus; IQR, interquartile range; MELD, Model for End-Stage Liver Disease; NA, not available; NAFLD, nonalcoholic fatty liver disease.

**REFERENCES**

1. Sun N, Lee YT, Zhang RY, et al. Purification of HCC-specific extracellular vesicles on nanosubstrates for early HCC detection by digital scoring. *Nat Commun* 2020;11:4489.
2. Thery C, Witwer KW, Aikawa E, et al. Minimal information for studies of extracellular vesicles 2018 (MISEV2018): a position statement of the International Society for Extracellular Vesicles and update of the MISEV2014 guidelines. *J Extracell Vesicles* 2018;7:1535750.
3. Lotvall J, Hill AF, Hochberg F, et al. Minimal experimental requirements for definition of extracellular vesicles and their functions: a position statement from the International Society for Extracellular Vesicles. *J Extracell Vesicles* 2014;3:26913.
4. Sun N, Tran BV, Peng Z, et al. Coupling lipid labeling and click chemistry enables isolation of extracellular vesicles for noninvasive detection of oncogenic gene alterations. *Advanced Science* 2022;In press.